Prediction of the Effective Diffusivity in Pore Networks Close to a Percolation Threshold

Lin Zhang and Nigel A. Seaton
Dept. of Chemical Engineering, University of Cambridge, Cambridge CB2 3RA, United Kingdom

The problem of diffusion in pore networks that are close to a percolation threshold is considered. Such networks arise: if the network is poorly connected; if the diffusing molecules are of a comparable size to the pores so that the fraction of the network accessible to the molecules is close to the percolation threshold; and in solids with multimodal pore-size distributions in which the pores belonging to the largest mode form a network close to the percolation threshold. We have investigated diffusion in such networks, using a new method in which the mass balance equations for diffusion on a regular lattice are solved using a Monte Carlo approach, coupled with a renormalized effective medium approximation. The method is accurate both close to and far from the percolation threshold, and is fast enough for routine calculations, such as in catalyst design applications.

Introduction

The problem of the prediction of the effective diffusivity of porous solids arises in the design of catalyst supports and adsorbents. For example, if the effective diffusivities of the species involved in a catalytic reaction can be predicted as a function of the morphology of the catalyst support, then an optimal pore structure can be identified. The prediction of the effective diffusivity depends, in the first place, on the availability of the appropriate experimental measurements. These include measurements of the bulk diffusion coefficients of the relevant species and determination of those aspects of the morphology of the solid that are amenable to analysis. These data must then be converted to an estimate of the effective diffusivity using a method that is both accurate and fast enough to repeat many times during the design process.

Sahimi et al. (1990) have reviewed methods for predicting the effective diffusivity of porous solids, as well as other aspects of transport and reaction in porous media. A realistic model of the pore network must incorporate both the geometry of the pores (the pore shape and the pore-size distribution) and the topology of the pore network. For reasons of tractability, it is convenient to map the real pore network onto a regular lattice. In this mapping, each pore becomes a bond on the lattice and each intersection between pores becomes a node. The mean coordination number of the lattice, which reflects the topology of the pore network, can be allowed to vary by deleting some of the bonds in the lattice or, equivalently, by setting their width to zero. Both parameters of this structural model, the mean coordination number and the pore-size distribution, can be obtained experimentally. The pore-size distribution can be obtained from nitrogen sorption measurements using the method of Barrett et al. (1951), its variants due to Cranston and Inkley (1957), Brunauer et al. (1967) and Broekhoff and de Boer (1967), or the statistical-mechanical method of Seaton et al. (1989). Recently, Seaton and coworkers (Seaton, 1991; Liu et al., 1992) have developed a method for determining the mean coordination number of a solid from sorption measurements.

If it is assumed that the pores in the network are much longer than they are wide, transport is essentially one-dimensional within the individual pores so that the calculation of the effective diffusivity is reduced to the solution of a set of linear equations (often called Kirchhoff's equations), each of which represents a mass balance at one of the nodes. If each bond on a lattice is associated with a particular pore size, chosen at random from the appropriate pore-size distribution, the mass-balance equations can be solved numerically to give the effective diffusivity. For convenience, we call this the direct solution (DS) method. The calculation must be repeated over many realizations of the lattice (with pore sizes distributed randomly in each case) to obtain a good value for the effective diffusivity. In addition, the effect of lattice size must be considered to eliminate the finite-size effect. The computer time

Correspondence concerning this article should be addressed to N. A. Seaton.

required for such calculations is large; for example, it typically requires many hours on a Sun SPARC Station 1^+ to obtain an accurate result. This suggests that while it is feasible to carry out a few such calculations, the large amount of computation required for the optimization of the pore structure would take too long with current computer technology. In practice, therefore, an approximate solution method is required.

Kirkpatrick (1973) obtained a solution to the analogous problem of calculating the effective conductivity of a network of conductors using an effective medium approximation (EMA). The EMA used by Kirkpatrick has been shown to be accurate provided the network is not near its percolation threshold (Kirkpatrick, 1973; Koplik, 1981). The failure of EMA near the percolation threshold reflects the poor estimate of the percolation threshold provided by EMA. For example, for bond percolation on a simple cubic lattice, EMA predicts that the percolation threshold, $p_c = 1/3$ which is much higher than the accurate value of 0.2493 (Stauffer and Zabolitzky, 1986). Several workers have exploited the analogy between diffusion and electrical conduction, and applied EMA to the prediction of effective diffusivities. Davis and coworkers (Davis et al., 1975; Davis, 1977) showed that EMA could be extended in a straightforward way to calculate the effective diffusivity of a pore network by replacing the electrical conductance with an equivalent diffusional conductance. Benzoni and Chang (1984) employed EMA to estimate the effective diffusivity of a pore network with a binary distribution of pore sizes. More recently, Burganos and Sotirchos (1987) and Sotirchos and Burganos (1988) established a rigorous basis for the application of EMA to the diffusion problem by deriving the correct relationship between the effective diffusional conductance obtained from EMA and the effective diffusivity of the pore network.

As EMA is accurate except near the percolation threshold, it is natural to ask whether networks close to the percolation threshold arise in practice. If this were not the case, EMA would be all that was required. The occurrence of a percolation transition in the desorption isotherm during nitrogen sorption experiments (Liu et al., 1992), which would not occur if the network were near its percolation threshold, suggests that for many solids the pore network is sufficiently well-connected for EMA to be applicable. Nevertheless, even for solids with well-connected pore networks, there are situations in which the ability to model diffusion near the percolation threshold is important. First, if the diffusing species are of a comparable size to the pores, some of the pores will be inaccessible to some of the species. The proportion of pores that are inaccessible will vary from species to species so that each species diffuses through a network with a different effective connectivity. Some species may experience a network that is close to its percolation threshold. The diffusion of molecules comparable in size to the pores has been considered in detail by Sahimi and Jue (1989) and by Sahimi (1992). Secondly, in some fluid-solid reactions (both catalytic and noncatalytic), the pore network evolves with time due to the growth or deposition of a solid phase. Examples of such processes are the deposition of metal sulfide in hydrodemetalation catalysts and the reaction of sulfur dioxide with calcined limestone. The reactivity of the solid is reduced as the solid is deposited, due both to the decreasing surface area and to the reduction in the effective diffusivity as pores are progressively reduced in size and then blocked by the solid. The resulting decrease in the connectivity of the network eventually leads to a percolation transition (Mohanty et al., 1982; Sahimi and Tsotsis, 1985; Mann et al., 1986; Mo and Wei, 1986; Reyes and Jensen, 1987; Shah and Ottino, 1987; Melkote and Jensen, 1989). The need to calculate the effective diffusivity near the percolation threshold is inherent to this type of process. Finally, in a solid with a multimodal pore-size distribution, transport will be dominated by the pores that form the largest mode of the distribution, provided that they form a percolating subnetwork and that the modes are sufficiently far apart. If the subnetwork formed by the pores in the largest mode is near the percolation threshold, the percolation behavior of that subnetwork will dominate the effective diffusivity of the whole network.

It is of interest to note that percolation concepts can sometimes be useful even when the network is in no physical sense close to a percolation threshold. Ambegaokar et al. (1971) pointed out that provided the distribution of conductances is broad, the effective transport properties of a network are dominated by the contribution of a barely-percolating subnetwork composed of the larger conductances. This idea is the basis of a method developed by Katz and Thompson (1986, 1987) for the prediction of the electrical conductivity and fluid permeability of oil reservoir rocks.

Sahimi et al. (1983) have combined elements of renormalization group theory with EMA to produce a method for calculating the effective conductivity that is more accurate near the percolation threshold than the original EMA. In this article, we present a new method for the prediction of the effective diffusivity of amorphous porous solids, based on the approach of Sahimi et al. We have used a Monte Carlo procedure to adapt their basic approach to predict the effective diffusivity of solids with continuous pore-size distributions (in their work, a binary conductance distribution was used). We demonstrate the accuracy of the method by comparing its predictions with essentially exact results from the direct numerical solution of the mass-balance equations describing diffusion on the simple cubic lattice. We go on to consider the variation in the rate of hindered diffusion as a function of molecule size and diffusion in solids with bimodal pore-size distributions.

Theory

The diffusional flux through a cylindrical pore with radius r and length l is given by:

$$J = \frac{\pi D(r) r^2}{l} \Delta c \tag{1}$$

where $D(r)$ is the diffusion coefficient of the diffusing species, and Δc is the difference in the concentration of that species over the length of the pore. By allowing the diffusion coefficient to vary with pore radius we allow for diffusion of the Knudsen and hindered types. By analogy with Ohm's law, the diffusional conductance, g, can be defined by:

$$g = \frac{\pi D(r) r^2}{l} = \frac{\pi}{l} a(r) \tag{2}$$

where for convenience, the pore-size-dependent factors are collected together in the quantity $a(r)=D(r)r^2$.

In the effective medium approximation (EMA) (Kirkpatrick, 1973), the network of conductances is replaced by an effective network in which each bond has the same conductance. The effective medium conductance, $<g>_{EMA}$, is the solution to:

$$\int h_g(g)\frac{(g-<g>_{EMA})}{[g+(Z/2-1)<g>_{EMA}]}dg=0 \tag{3}$$

where Z is the coordination number of the network, and $h_g(g)$ is the conductance probability density function [that is, the number fraction of pores with a diffusional conductance between g and $g+dg$ is $h_g(g)dg$]. For a network in which the mean coordination number is reduced from that of the original network by the random removal of bonds,

$$h_g(g)=(1-p)\delta(g)+pf_g(g) \tag{4}$$

where $\delta(g)$ is the Dirac delta function, and p is the bond occupation probability (that is, the fraction of bonds not deleted).

For the diffusion problem, it is convenient to rewrite Eq. 3 in terms of $a(r)$ as follows:

$$\int h_r(r)\frac{[a(r)-<a>_{EMA}]}{[a(r)+(Z/2-1)<a>_{EMA}]}dr=0 \tag{5}$$

where $h_r(r)$ is the pore-size distribution (strictly the probability density function for the pore radius), and $<a>_{EMA}$ is the effective medium value of $a(r)$. In writing Eq. 5, we have assumed that the pores are of uniform length, l_u. For a network diluted by the random removal of bonds,

$$h_r(r)=(1-p)\delta(r)+pf_r(r) \tag{6}$$

where $f_r(r)$ is the pore-size distribution of the surviving pores in a diluted network. Burganos and Sotirchos (1987) have shown that for a network of cylindrical pores, the effective diffusivity, D_e, is related to $<a>_{EMA}$ by:

$$D_e=\frac{1}{3}K\pi l_u<a>_{EMA} \tag{7}$$

where K is the number of pores per unit volume of the solid. K is given by (Burganos and Sotirchos, 1987):

$$K=\frac{\epsilon}{\pi<r^2>l_u} \tag{8}$$

where ϵ is the porosity of the solid, so that

$$D_e=\frac{1}{3}\epsilon\frac{<a>_{EMA}}{<r^2>} \tag{9}$$

where $<r^2>$ is the arithmetical mean value of r^2.

$$<r^2>=\int_0^\infty f_r(r)r^2\,dr \tag{10}$$

In position space renormalization group (PSRG) theory (Stinchcombe and Watson, 1976; Bernasconi, 1978; Reynolds et al., 1980; Tsallis et al., 1983; Shah and Ottino, 1986), the original network is divided into identical unit cells of linear dimension b. Figure 1a shows such a unit cell with $b=2$ for a simple cubic network. The conductances of the bonds are distributed according to the conductance distribution $h_g(g)$: that is, the bonds are absent with probability $(1-p)$, and the remaining bonds are assigned conductances from the distribution $f_g(g)$. The renormalization procedure involves replacing the original cell by three renormalized bonds (Figure 1b). The conductance distribution of the renormalized bonds, $f'_g(g)$, is chosen so that the three normalized bonds offer the same resistance to transport as the original cell. That is, if a potential difference (or a concentration difference) were applied in turn across a

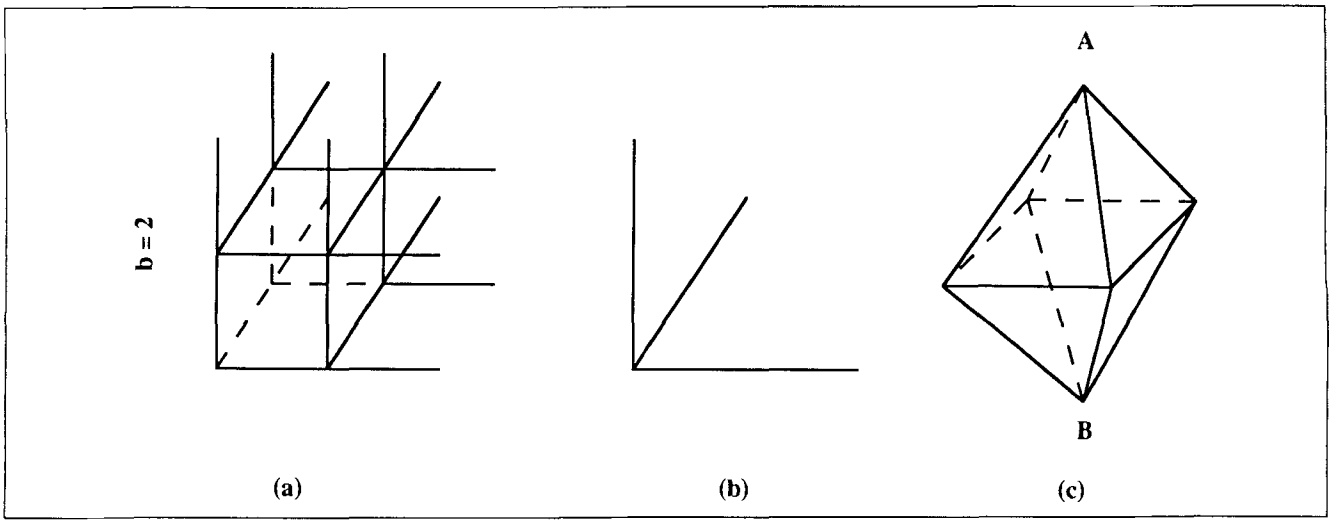

Figure 1. (a) $b=2$ renormalization cell for the simple cubic lattice; (b) renormalized bonds corresponding to this cell; and (c) equivalent electrical circuit.

large number of replicas of the original cell (in the x-direction, say) with the conductances being assigned at random from $f_g(g)$, the measured distribution of currents would be the same as those calculated from the conductance distribution of the renormalized bonds. Note that the unit cell of Figure 1a is equivalent to the electrical circuit (a generalized Wheatstone bridge) with 12 bonds shown in Figure 1c. The fraction of occupied bonds changes on renormalization. Figure 2 shows the renormalized bond occupation probability, $R(p)$, vs. p for the renormalization cell of Figure 1a. Thus, on renormalization, the original conductance distribution $h_g(g) = (1-p)\delta(g) + pf_g(g)$ is replaced by $h_g'(g) = [1-R(p)]\delta(g) + R(p)f_g'(g)$.

A new cell, topologically equivalent to the original but with linear dimension a factor of b larger, is then created out of the renormalized bonds, and the renormalization procedure is repeated. With each successive renormalization, the conductance distribution becomes increasingly narrow. As the number of realizations $\to\infty$, $h_g'(g) \to \delta(g-\hat{g})$ where $\hat{g}$ is the renormalization group estimate of the effective conductance. At the same time, the fraction of occupied bonds moves toward one of three fixed points. If the initial fraction of occupied bonds satisfies $p^* = R(p^*)$, the fraction of occupied bonds does not change as a result of renormalization, and p^* is an estimate of percolation threshold p_c. For the renormalization cell of Figure 1, $p^* = 0.2085$ (Bernasconi, 1978), compared with the correct value of $p_c = 0.2493$ (Stauffer and Zabolitzky, 1986). If $p > p^*$, the fraction of occupied bonds increases with each renormalization step and tends to unity. If $p < p^*$, the fraction of occupied bonds decreases with each renormalization step and tends to zero. Thus, with each renormalization, the system moves further from the percolation threshold.

The renormalized conductance distribution $h_g'(g)$ is given by the solution of (Stinchcombe and Watson, 1976):

$$h_g'(g) = [1-R(p)]\delta(g) + R(p)f_g'(g)$$

$$= \int\int\cdots\int h_g(g_1)h_g(g_2), \ldots, h_g(g_n)dg_1dg_2\ldots dg_n\,\delta(g-g') \tag{11}$$

where $g_1, g_2, \ldots, g_n$ are the individual conductances in the electrical circuit (Figure 1c) that is equivalent to the renormalization cell (Figure 1a), and g' is the conductance of this circuit. g' can be obtained analytically as a function of $g_1, g_2, \ldots, g_n$ by solving Kirchhoff's equations for the circuit.

Stinchcombe and Watson (1976) solved Eq. 11 exactly for a two-dimensional renormalization cell. In general, however, an exact solution cannot be obtained, and it is necessary to adopt an alternative approach. One approach (Stinchcombe and Watson, 1976; Bernasconi, 1978; Tsallis et al., 1983) for a binary conductance distribution, $h_g(g) = (1-p)\,\delta(g) + p\delta(g-g_0)$, is to replace the renormalized distribution $h_g'(g)$ with an appropriately chosen renormalized binary distribution. A second approach, which is applicable to continuous as well as discrete conductance distributions, is to solve Eq. 11 using a Monte Carlo technique (Bernasconi, 1978). This approach, however, is too time-consuming to be suitable for the routine calculations.

The observation that the effective medium approximation is accurate except close to the percolation threshold and that a renormalized network is further from the percolation threshold than the original network led Sahimi et al. (1983) to combine the EMA and the PSRG approaches. In their approach,

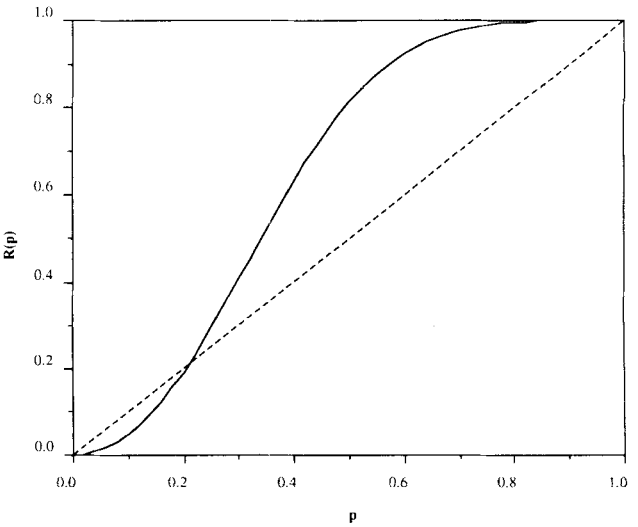

Figure 2. Renormalized bond occupation probability, *R(p)*, vs. the original bond occupation probability, *p*.

known as the renormalized effective medium approximation (REMA), a single renormalization step is carried out and the renormalized conductance distribution $h_g'(g)$ is used as the input to EMA (Eq. 3) instead of the original distribution $h_g(g)$. Sahimi et al. applied REMA to a binary conductance distribution on the square and simple cubic lattices and compared the results with the original EMA and with the direct solution (DS) method. They found that REMA was much superior to EMA in the region of the percolation threshold. In particular, for a simple cubic lattice, percolation occurs when $R(p) = 1/3$ which leads, via the relationship between $R(p)$ and p (Bernasconi, 1978), to $p_c = 0.2673$. The REMA value of the percolation threshold is thus much closer to the true value of 0.2493 than either the PSRG value of 0.2085 or the EMA value of 1/3.

Sahimi (1988) tackled the prediction of the fluid permeability of a solid having a continuous pore-size distribution. He used REMA, with the renormalization cell shown in Figure 1, to predict the relative permeability of a model porous solid. To make REMA calculation tractable, Sahimi discretized the distribution, thereby converting the integration of Eq. 3 to a summation. By making a comparison with a numerical solution to Eq. 11, he found for the particular conductance distribution used in his calculations that six discrete conductances gave an adequate representation of the original continuous distribution. Although the discretization procedure worked well in this particular case, the number of discrete conductances required to give good results must vary from distribution to distribution and would not be known *a priori*. The choice of the values of the discrete conductances and their associated weights is also problematical. As a result, the suitability of a particular discretization scheme cannot be assessed without carrying out the full numerical calculation. More recently, Petropolous et al. (1991) have adopted a discretization approach to the application of REMA to continuous conductance distributions in a two-dimensional square lattice.

We have adapted the basic REMA approach of Sahimi et al. (1983) for the prediction of the effective diffusivity of porous solids with continuous pore-size distributions. Our ap-

proach involves a Monte Carlo procedure in which conductances are chosen at random from the conductance distribution, $h_g(g)$, and assigned to the bonds of the unit cell shown in Figure 1a. The renormalized conductance corresponding to this assignment of conductances is then calculated. This procedure is repeated over many realizations of the unit cell to give the renormalized conductance distribution, $h_g'(g)$, which is then the input to the EMA. It is convenient to work in terms of the quantity a defined in Eq. 2 and the pore-size distribution $h_r(r)$ rather than with g and $h_g(g)$.

The Monte Carlo simulation method (which for convenience we call MC-REMA) is described in detail as follows. In each realization of the unit cell, every bond in the equivalent electrical circuit of Figure 1c is labeled as occupied with probability p, or unoccupied with probability $(1-p)$. If it is occupied, it is assigned a pore size randomly from $f_r(r)$. The renormalized conductance for each realization is calculated using the solution to the mass-balance equations for the circuit of Figure 1c, which is given in the Appendix. In this calculation, caution is required in dealing with the unoccupied bonds. If a cluster of one or more occupied bonds is not attached to either end of the equivalent electrical circuit, the potentials of the nodes in that cluster are indeterminate and the conductance matrix is singular. To avoid this problem, the unoccupied bonds are assigned a small conductance, chosen so that it is much smaller than any of the real conductances in the network. This procedure has a negligible effect on the calculated renormalized conductance g'. The output of the Monte Carlo procedure is a set of renormalized conductances, which is then used as the input to EMA. If a_i' is the renormalized value of quantity a (as defined in Eq. 2) for realization i, Eq. 5 becomes:

$$\frac{1}{N}\sum_{i}^{N}\frac{(a_i' - <a'>_{\text{EMA}})}{[a_i' + (Z/2-1)<a'>_{\text{EMA}}]} = 0 \tag{12}$$

where N is the number of realizations of the renormalization cell.

The effective diffusivity is obtained by rewriting Eq. 7 with $<a'>_{\text{EMA}}$ in place of $<a>_{\text{EMA}}$ and $2l_u$ in place of l_u (as each renormalized bond is twice as long as the original).

$$D_e = \frac{1}{3}K'\pi(2l_u)<a'>_{\text{EMA}} \tag{13}$$

where K' is the number of pores per unit volume in the renormalized network. The number of pores per unit volume decreases by a factor of eight on renormalization so

$$K' = \frac{1}{8}\frac{\epsilon}{\pi<r^2>l_u} \tag{14}$$

Finally, by substituting Eq. 14 into Eq. 13, the effective diffusivity is given by:

$$D_e = \frac{1}{12}\epsilon\frac{<a'>_{\text{EMA}}}{<r^2>} \tag{15}$$

Results and Discussion

To evaluate the accuracy of the MC-REMA predictions, it is necessary to generate essentially exact results for the effective diffusivity of a simple cubic lattice using the DS method. By "essentially exact," we mean here that the error can be made arbitrarily small by the expenditure of computer time, that is, by studying large lattices and by carrying out many realizations. As in the MC-REMA calculation, the bonds are randomly removed with probability $(1-p)$ with a radius being assigned to the surviving bonds from the pore-size distribution $f_r(r)$, and many realizations are carried out. The following mass balance must be satisfied at each node in the lattice:

$$\sum_i J_i = 0 \tag{16}$$

where the summation is over all pores that meet at that node. Substituting Eq. 1 in Eq. 16 gives:

$$\sum_i \frac{\pi D(r) r^2}{l}\Delta c_i = 0 \tag{17}$$

A concentration difference is imposed in the x-direction. Periodic boundary conditions are imposed in the y- and z-directions so that, for example, a flux leaving the lattice from a node on the $y=L$ face (where L is the linear dimension of the lattice, expressed as a number of pore lengths) re-enters through the corresponding node on the $y=0$ face. The mass-balance equations for all the internal nodes, together with the specifications of the concentrations on the $x=0$ and $x=L$ surfaces, can be written in matrix form as:

$$\underline{\underline{A}}\,\underline{c} = \underline{b} \tag{18}$$

where $\underline{c}$ is a vector containing the concentrations at the nodes. We have used an iterative method (the Lanczos algorithm, implemented in the numerical algorithms group subroutine F04QAF) to solve Eq. 18 for the concentration vector $\underline{c}$. As in the MC-REMA calculation, a very small conductance is assigned to the deleted bonds in order to prevent $\underline{\underline{A}}$ from becoming singular if isolated clusters of bonds are present. Once the concentrations have been calculated, the flux across the lattice and hence the effective diffusion coefficient can be obtained.

We have compared the results from the DS method with MC-REMA for two diffusion mechanisms: molecular and Knudsen. The Knudsen diffusion coefficient is proportional to the pore radius r:

$$D_K = \frac{2}{3}\left(\frac{8RT}{\pi M}\right)^{1/2} r \tag{19}$$

where R is the gas constant, T is the temperature, and M is the molecular weight of the diffusing species.

In our comparison of the effective diffusivity obtained from the DS method with the predictions of MC-REMA, we have used a lognormal pore-size distribution (as distributions of approximately this form are often found experimentally). The lognormal distribution takes the form:

$$f_r(r) = \frac{1}{\sqrt{2\pi}\,\sigma r}\exp\left\{-\frac{[\ln(r)-\mu]^2}{2\sigma^2}\right\} \tag{20}$$

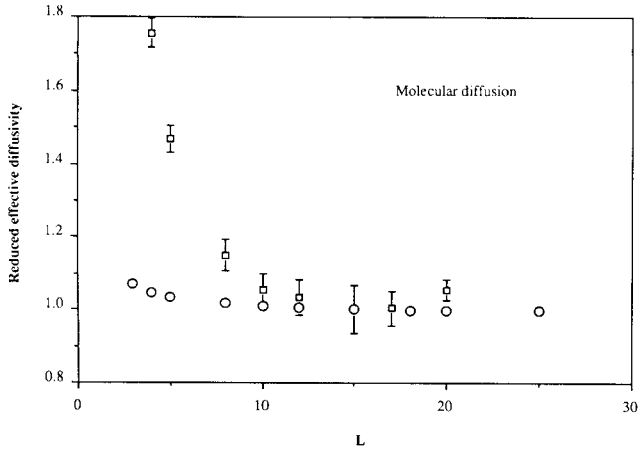

Figure 3. Network size dependence of DS results for molecular diffusion at two bond occupancy probabilities: $p = 1.0$ (○) and $p = 0.35$ (□).

In each case, the effective diffusivity is reduced by its value at $L = 15$. $m = 40$ Å and $s = 24$ Å. Error bars are shown where the error is larger than the symbol.

where μ and σ are parameters. The mean, m, and the standard deviation, s, of the distribution are given by:

$$m = \exp(\mu + 0.5\sigma^2) \tag{21}$$

and

$$s = [\exp(2\mu + 2\sigma^2) - m^2]^{1/2} \tag{22}$$

As it is desired to predict the effective diffusivity of very large (essentially infinite) systems, the effect of finite system size must be effectively eliminated from results of the DS calculations. Figure 3 shows the variation of the effective diffusivity with lattice size, L, for molecular diffusion with two bond occupation probabilities, $p = 1$ and $p = 0.35$. The effective diffusivity is reduced by the values at $L = 15$. The calculated diffusivities are higher for small network size and approach a constant value as the size increases. From Figure 3 it can be seen that the influence of network size on the simulation results is very small for $L \geq 15$.

The reduced effective diffusivities predicted by EMA and MC-REMA are compared with the DS results for a given pore-size distribution in Figures 4a and 4b, which show molecular and Knudsen diffusion, respectively. A large number of realizations are required in calculating the renormalized conductance distribution from the equivalent electrical circuit (Figure 1c). In the MC-REMA calculations for Figure 4a and 4b, 200,000 realizations were performed. However, the error introduced by carrying out only 10 thousand realizations is less than 1%, so this lower number of realizations may be sufficient for practical purposes. EMA is accurate for $0.6 < p < 1.0$, but becomes progressively less so, as the percolation threshold is approached, reflecting the poor estimate of the percolation threshold with EMA. MC-REMA, on the other hand, is much more accurate near the percolation threshold, while its accuracy is comparable to that of EMA far from p_c. Using a Sun SPARC Station 1^+, MC-REMA required of the order of a minute per ten thousand realizations. MC-REMA

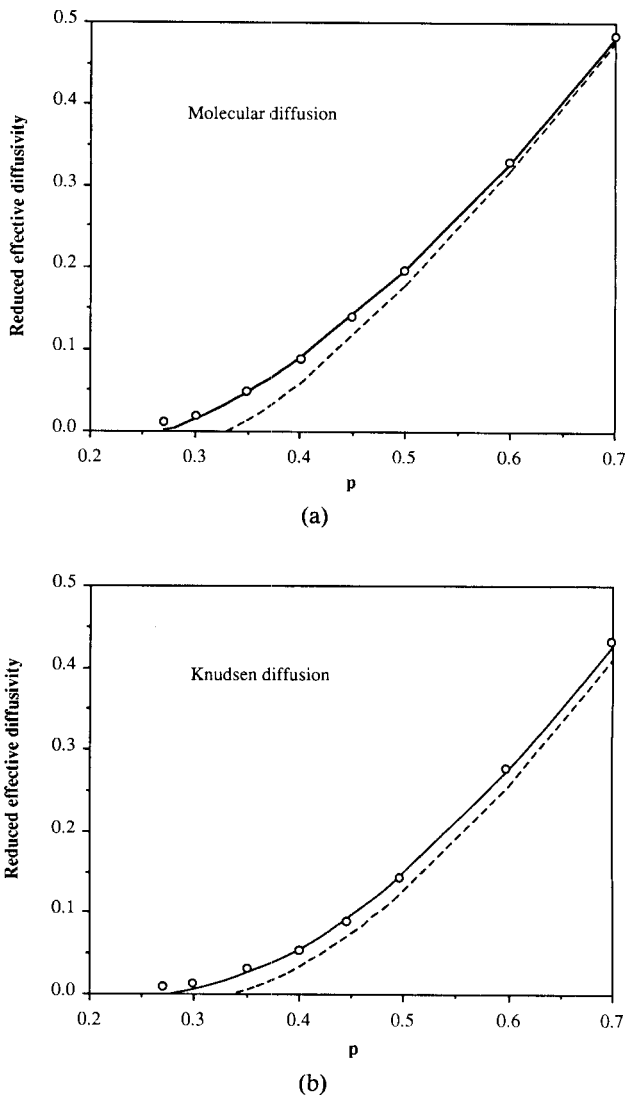

Figure 4. Comparison of effective diffusivities predicted by MC-REMA, EMA, and DS: (a) molecular diffusion and (b) Knudsen diffusion.

The effective diffusivities are reduced by their values at $p = 1.0$. ○ = DS; —— = MC-REMA; ----- = EMA. $m = 40$ Å and $s = 24$ Å.

is thus two orders of magnitude faster than the DS method; this reflects the fact that MC-REMA effectively involves the calculation of the conductance of a network of 12 bonds compared with thousands of bonds in the DS method.

Having established the accuracy of MC-REMA, we consider its application to hindered diffusion as a function of molecular size and to diffusion in networks with a bimodal pore-size distribution. We model hindered diffusion using the diffusion coefficient of Spry and Sawyer (1975):

$$D_h = D_m\left(1 - \frac{r_{mol}}{r}\right)^4 \tag{23}$$

for $r_{mol} < r$, where D_m is the molecular diffusion coefficient and r_{mol} is the molecular radius.

As the molecular radius increases, the fraction of the network accessible to the molecule decreases until at a critical

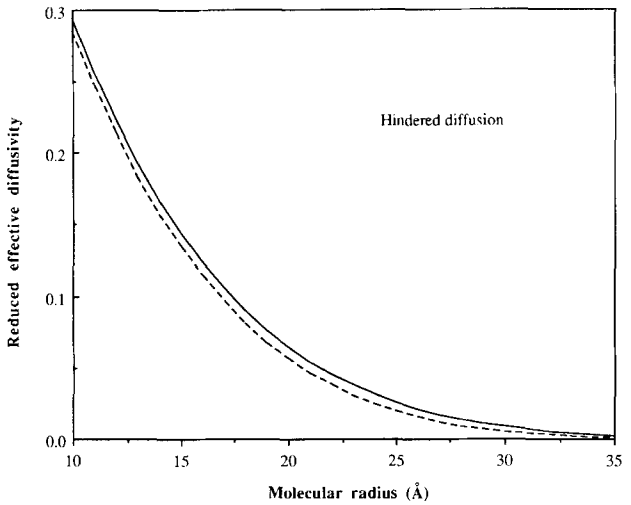

Figure 5. Effective diffusivity vs. molecular radius for hindered diffusion.

The effective diffusivity is reduced by its value at zero molecular radius. —— = MC-REMA; ---- = EMA. $m = 40$ Å and $s = 24$ Å.

radius the percolation threshold is reached. Molecules larger than this critical size cannot diffuse through the network. Figure 5 shows a comparison between the predictions of MC-REMA and EMA for hindered diffusion as a function of molecular radius. While MC-REMA and EMA give similar results for small molecules (far from the percolation threshold), the results are significantly different as the percolation threshold is approached.

We represent a bimodal pore-size distribution by the sum of the lognormal distributions:

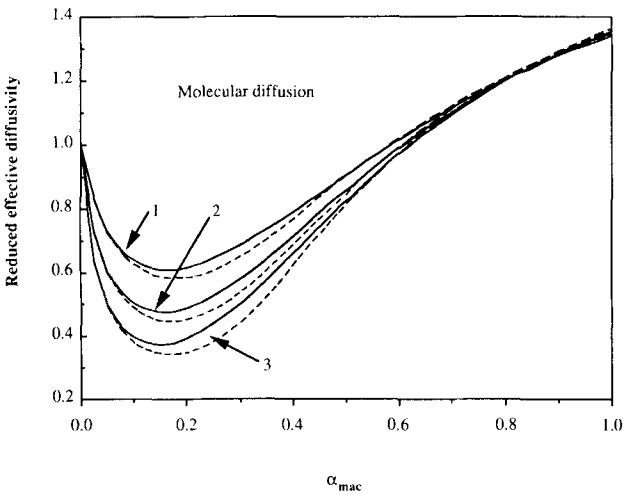

Figure 6. Comparison of the effective diffusivity predicted by MC-REMA with that predicted by EMA for a bimodal pore-size distribution.

Effective diffusivities are reduced by the results of $\alpha_{mac} = 0$. —— = MC-REMA; ---- = EMA. The mean pore radius of the macropore mode is 160 Å (1), 200 Å (2), and 240 Å (3). In all the calculations, the mean pore radius of the micropore mode is 40 Å. The standard deviation is 20 Å for both modes.

$$f_r(r) = \frac{\alpha_{mic}}{\sqrt{2\pi}\,\sigma_{mic} r} \exp\left\{-\frac{[\ln(r) - \mu_{mic}]^2}{2\sigma_{mic}^2}\right\} + \frac{\alpha_{mac}}{\sqrt{2\pi}\,\sigma_{mac} r} \exp\left\{-\frac{[\ln(r) - \mu_{mac}]^2}{2\sigma_{mac}^2}\right\} \quad (24)$$

where

$$\alpha_{mic} + \alpha_{mac} = 1 \quad (25)$$

Provided the micropore and macropore distributions are sufficiently far apart that the two lognormal functions do not overlap, the number fractions of pores in these modes are given by α_{mic} and α_{mac}, respectively.

Figure 6 shows a comparison of the effective diffusivities predicted by MC-REMA and EMA as a function of the fraction of macropores, α_{mac}, holding the porosity constant. The effective diffusivities are normalized by the result for $\alpha_{mac} = 0$. As α_{mac} is increased from 0 to 1, the effective diffusivity goes through a minimum. This can be understood as follows. As α_{mac} is increased from zero (holding the porosity constant), some of the micropores are replaced by a smaller number of macropores. The macropores are isolated from each other and contribute little to diffusion. The main effect of increasing α_{mac} is therefore to reduce the number of pores per unit volume and hence the effective diffusivity. However, when the number of macropores in the network has reached a stage where some larger clusters of macropores are formed, the effect of macropores on the effective diffusivity becomes important. Finally, when a percolating cluster of macropores is formed, it dominates the diffusion process. It can be seen from Figure 6 that EMA significantly underestimates the effective diffusivity over a wide range of values of α_{mac}. Furthermore, as the two modes move further apart, the EMA predictions are increasingly at variance with those of the more accurate MC-REMA.

Summary

We have investigated diffusion in amorphous, porous solids which have pore networks close to the percolation threshold, using the MC-REMA method. This method is accurate both close to and far from the percolation threshold and is fast, requiring of the order of one minute on a modern workstation. We have demonstrated the superiority of MC-REMA over the conventional EMA in two cases which are likely to be of practical importance: hindered diffusion and diffusion in solids with a multimodal pore-size distribution.

Acknowledgment

This work was funded by a grant from the Interfaces and Catalysis Initiative of the United Kingdom Science and Engineering Research Council. L.Z. gratefully acknowledges a scholarship from the Cambridge Overseas Trust.

Notation

a = a factor of the diffusional conductance, defined in Eq. 2
$\underline{\underline{A}}$ = matrix of coefficients in the DS method
$\underline{b}$ = constant vector in the DS method
c = nodal concentration
$\underline{c}$ = nodal concentration vector
D_e = effective diffusivity

D_h = hindered diffusion coefficient
D_k = Knudsen diffusion coefficient
D_m = molecular diffusion coefficient
$D(r)$ = generalized diffusion coefficient
$f_g(g)$ = conductance distribution (occupied bonds only)
$f_r(r)$ = pore-size distribution (occupied bonds only)
g = bond conductance
$\hat{g}$ = effective conductance calculated using PSRG method
g_0 = conductance in a binary distribution
G = variable defined in the Appendix
$h_g(g)$ = conductance distribution (including unoccupied bonds)
$h_r(r)$ = pore-size distribution (including unoccupied bonds)
J = diffusional flux
K = number of pores per unit volume
l = pore length
l_u = uniform pore length
L = network size expressed as a number of pore lengths
M = molecular weight of diffusing species
m = mean of lognormal distribution
N = number of realizations of the renormalization cell
p = bond occupation probability
p_c = percolation threshold
p^* = fixed point probability
R = gas constant
$R(p)$ = bond occupation probability in renormalized network
r = pore radius
r_{mol} = molecular radius
s = standard deviation of lognormal distribution
T = temperature
V_i = potential of node i in the equivalent circuit
Z = mean coordination number

Greek letters

α = number fraction of pores in one mode of a bimodal distribution
ϵ = porosity
μ = parameter of the lognormal distribution
σ = parameter of the lognormal distribution

Subscripts

EMA = effective quantities calculated using the effective medium approximation
mic = parameter of micropore distribution
mac = parameter of macropore distribution

Superscripts

* = renormalized variables

Literature Cited

Ambegaokar, V., B. I. Halperin, and J. S. Langer, "Hopping Conductivity in Disordered Systems," *Phys. Rev.*, **B4**, 2612 (1971).

Barrett, E. P., L. G. Joyner, and P. H. Halenda, "The Determination of Pore Volume and Area Distributions in Porous Substances: I. Computations from Nitrogen Isotherms," *J. Amer. Chem. Soc.*, **73**, 373 (1951).

Benzoni, J., and H. C. Chang, "Effective Diffusion in Bidisperse Media—An Effective Medium Approach," *Chem. Eng. Sci.*, **39**, 161 (1984).

Bernasconi, J., "Real-Space Renormalization of Bond-Disordered Conductance Lattices," *J. Phys. Rev.*, **B18**, 2185 (1978).

Broekhoff, J. C. P., and J. H. de Boer, "Calculation of Pore Distributions from the Adsorption Branch of Nitrogen Sorption Isotherms in the Case of Open Cylindrical Pores," *J. Cat.*, **9**, 8 (1967).

Brunauer, S., R. Sh. Mikhail, and E. E. Bodor, "Pore Structure Analysis without a Pore Shape Model," *J. Colloid Interf. Sci.*, **24**, 451 (1967).

Burganos, V. N., and S. V. Sotirchos, "Diffusion in Pore Networks: Effective Medium Theory and Smooth Field Approximation," *AIChE J.*, **33**, 1678 (1987).

Cranston, R. W., and F. A. Inkley, "The Determination of Pore Structures from Nitrogen Adsorption Isotherms," *Adv. Catal.*, **9**, 143 (1957).

Davis, H. T., "The Effective Medium Theory of Diffusion in Composite Media," *J. Amer. Ceram. Soc.*, **60**, 499 (1977).

Davis, H. T., L. R. Valencourt, and C. E. Johnson, "Transport Processes in Composite Media," *J. Amer. Ceram. Soc.*, **58**, 446 (1975).

Katz, A. J., and A. H. Thompson, "A Quantitative Prediction of Permeability in Porous Rock," *Phys. Rev.*, **B34**, 8179 (1986).

Katz, A. J., and A. H. Thompson, "Prediction of Rock Electrical Conductivity from Mercury Injection Measurements," *J. Geophys. Res.*, **92**, 599 (1987).

Kirkpatrick, S., "Percolation and Conduction," *Rev. Mod. Phys.*, **45**, 574 (1973).

Koplik, J., "On the Effective Medium Theory of Random Linear Networks," *J. Phys. C: Solid State Phys.*, **14**, 4821 (1981).

Liu, H., L. Zhang, and N. A. Seaton, "Determination of the Connectivity of Porous Solids from Nitrogen Sorption Measurements: II. Generalisation," *Chem. Eng. Sci.*, in press (1992).

Mann, R., P. M. Sharratt, and G. Thomson, "Deactivation of a Supported Zeolite Catalyst: Diffusion Reaction and Coke Deposition in Stochastic Pore Networks," *Chem. Eng. Sci.*, **41**, 711 (1986).

Melkote, R. R., and K. F. Jensen, "Models for Catalytic Pore Plugging: Application to Hydrodemetalation," *Chem. Eng. Sci.*, **44**, 649 (1989).

Mo, W. T., and J. Wei, "Effective Diffusivity in Partially Blocked Zeolite Catalyst," *Chem. Eng. Sci.*, **41**, 703 (1986).

Mohanty, K. K., J. M. Ottino, and H. T. Davis, "Reaction and Transport in Disordered Media: Introduction of Percolation Concepts," *Chem. Eng. Sci.*, **37**, 905 (1982).

Petropoulos, J. H., J. K. Petrou, and A. I. Liapis, "Network Model Investigation of Gas Transport in Bidisperse Porous Adsorbents," *Ind. Eng. Chem. Res.*, **30**, 1281 (1991).

Reyes, S., and K. F. Jensen, "Percolation Concepts in Modelling of Gas-Solid Reactions: III. Application to Sulphation of Calcined Limestone," *Chem. Eng. Sci.*, **42**, 565 (1987).

Reynolds, P. J., H. E. Stanley, and W. Klein, "Large-Cell Monte Carlo Renormalization Group for Percolation," *Phys. Rev.*, **B21**, 1223 (1980).

Sahimi, M., B. D. Hughes, L. E. Scriven, and H. T. Davis, "Real-Space Renormalization and Effective-Medium Approximation to the Percolation Conduction Problem," *Phys. Rev.*, **B28**, 307 (1983).

Sahimi, M., "On the Determination of Transport Properties of Disordered Systems," *Chem. Eng. Comm.*, **64**, 177 (1988).

Sahimi, M., "Transport of Macromolecules in Porous Media," *J. Chem. Phys.*, **96**, 4718 (1992).

Sahimi, M., G. R. Gavalas, and T. T. Tsotsis, "Statistical and Continuum Models of Fluid-Solid Reactions in Porous Media," *Chem. Eng. Sci.*, **45**, 1443 (1990).

Sahimi, M., and V. L. Jue, "Diffusion of Large Molecules in Porous Media," *Phys. Rev. Lett.*, **62**, 629 (1989).

Sahimi, M., and T. T. Tsotsis, "A Percolation Model of Catalyst Deactivation by Site Coverage and Pore Blockage," *J. Catal.*, **96**, 552 (1985).

Seaton, N. A., "Determination of the Connectivity of Porous Solids from Nitrogen Measurements," *Chem. Eng. Sci.*, **8**, 1895 (1991).

Seaton, N. A., J. P. R. B. Walton, and N. Quirke, "A New Analysis Method for the Determination of the Pore Size Distribution of Porous Carbons from Nitrogen Sorption Measurements," *Carbon*, **27**, 853 (1989).

Shah, N., and J. M. Ottino, "Effective Transport Properties of Disordered Multiphase Composites: Application of Real-Space Renormalization Group Theory," *Chem. Eng. Sci.*, **41**, 283 (1986).

Shah, N., and J. M. Ottino, "Transport and Reaction in Evolving, Disordered Composite: II. Coke Deposition in a Catalytic Pellet," *Chem. Eng. Sci.*, **42**, 73 (1987).

Sotirchos, S. V., and V. N. Burganos, "Analysis of Multicomponent Diffusion in Pore Networks," *AIChE J.*, **34**, 1106 (1988).

Spry, J. C. Jr., and W. H. Sawyer, "Configurational Diffusion Effects in Catalytic Demetalization of Petroleum Fractions," Paper 30C, AIChE Meeting, Los Angeles (1975).

Stauffer, D., and J. G. Zabolitzky, "Re-examination of 3D Percolation Threshold Estimates," *J. Phys. A: Math. Gen.*, **19**, 3705 (1986).

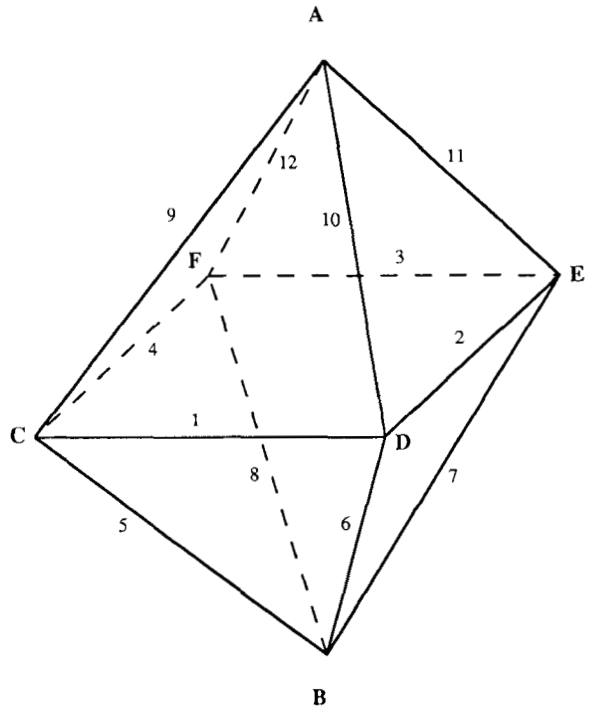

Figure 7. Labeling of bonds in the equivalent circuit.

Stinchcombe, R. B., and B. P. Watson, "Renormalization Group Approach for Percolation Conductivity," *J. Phys. C: Solid State Phys.*, **9**, 3221 (1976).

Tsallis, C., A. Coniglio, and S. Redner, "Break-Collapse Method for Resistor Networks and a Renormalisation-Group Application," *J. Phys. C: Solid State Phys.*, **16**, 4339 (1983).

Appendix

The 12 conductances in the equivalent circuit (Figure 1c) of the renormalization cell are labeled $g_1, g_2, \ldots, g_{12}$ (as shown in Figure 7). The conductance of the circuit is calculated by imposing a unit potential difference across the cell between nodes A and B and writing current balance equations for the four internal nodes C, D, E and F. The four equations are solved for V_C, V_D, V_E and V_F giving:

$$V_C=\frac{1}{G}\{g_9\{(g_2+g_1+g_6+g_{10})[(g_3+g_2+g_7+g_{11})(g_4+g_3+g_8+g_{12})-g_3^2]-g_2^2(g_4+g_3+g_8+g_{12})\}+g_{10}\{g_2g_3g_4+g_1(g_3+g_2+g_7+g_{11})(g_4+g_3+g_8+g_{12})-g_1g_3^2\}+g_{11}\{g_1g_2(g_4+g_3+g_8+g_{12})+g_3g_4(g_2+g_1+g_6+g_{10})\}+g_{12}\{g_1g_2g_3+g_4[(g_2+g_1+g_6+g_{10})(g_3+g_2+g_7+g_{11})-g_2^2]\}\} \quad \text{(A1)}$$

$$V_D=\frac{1}{D}\{g_9\{g_2g_3g_4+g_1[(g_3+g_2+g_7+g_{11})(g_4+g_3+g_8+g_{12})-g_3^2]\}+g_{10}\{(g_3+g_2+g_7+g_{11})[(g_1+g_4+g_5+g_9)(g_4+g_3+g_8+g_{12})-g_4^2]-g_3^2(g_1+g_4+g_5+g_9)\}+g_{11}\{g_1g_3g_4+g_2[(g_1+g_4+g_5+g_9)(g_4+g_3+g_8+g_{12})-g_4^2]\}+g_{12}\{g_2g_3(g_1+g_4+g_5+g_9)+g_1g_4(g_3+g_2+g_7+g_{11})\}\} \quad \text{(A2)}$$

$$V_E=\frac{1}{G}\{g_9\{g_1g_2(g_4+g_3+g_8+g_{12})+g_3g_4(g_2+g_1+g_6+g_{10})\}+g_{10}\{g_1g_3g_4+g_2[(g_1+g_4+g_5+g_9)(g_4+g_3+g_8+g_{12})-g_4^2]\}+g_{11}\{(g_4+g_3+g_8+g_{12})[(g_2+g_1+g_6+g_{10})(g_1+g_4+g_5+g_9)-g_1^2]-g_4^2(g_2+g_1+g_6+g_{10})\}+g_{12}\{g_1g_2g_4+g_3[(g_2+g_1+g_6+g_{10})(g_1+g_4+g_5+g_9)-g_1^2]\}\} \quad \text{(A3)}$$

and

$$V_F=\frac{1}{G}\{g_9\{g_1g_2g_3+g_4[(g_2+g_1+g_6+g_{10})(g_3+g_2+g_7+g_{11})-g_2^2]\}+g_{10}\{g_2g_3(g_1+g_4+g_5+g_9)+g_1g_4(g_3+g_2+g_7+g_{11})\}+g_{11}\{g_1g_2g_4+g_3[(g_2+g_1+g_6+g_{10})(g_1+g_4+g_5+g_9)-g_1^2]\}+g_{12}\{(g_1+g_4+g_5+g_9)[(g_3+g_2+g_7+g_{11})(g_2+g_1+g_6+g_{10})-g_2^2]-g_1^2(g_3+g_2+g_7+g_{11})\}\} \quad \text{(A4)}$$

where

$$G=-2g_1g_2g_3g_4+g_1^2[g_3^2-(g_3+g_2+g_7+g_{11})(g_4+g_3+g_8+g_{12})]-(g_1+g_4+g_5+g_9)[g_3^2(g_2+g_1+g_6+g_{10})+g_2^2(g_4+g_3+g_8+g_{12})]+g_4^2[g_2^2-(g_2+g_1+g_6+g_{10})(g_3+g_2+g_7+g_{11})]+(g_1+g_4+g_5+g_9)(g_2+g_1+g_6+g_{10})(g_3+g_2+g_7+g_{11})(g_4+g_3+g_8+g_{12}) \quad \text{(A5)}$$

The conductance g' of the renormalization cell is given by:

$$g'=g_5V_C+g_6V_D+g_7V_E+g_8V_F$$

Manuscript received Feb. 28, 1992, and revision received June 18, 1992.